RSC Advances

PAPER

View Article Online
View Journal | View Issue

Cite this: *RSC Adv.*, 2026, **16**, 26372

Hydrophobic modification of a polyurethane sponge *via* emulsion polymerization for selective oil–water separation

Md. Ariful Islam Setu,[a] Md. Rezaul Haque,[a] Md. Suzon Ahmed,[a] Ahmed B. M. Ibrahim,[b] Muhammad Sarwar Hossain [a] and Md. Kamrul Hasan *[a]

A conventional polyurethane (PU) sponge shows less selectivity, which restricts its ability to favorably absorb oils. To address this limitation, the sponge surface was engineered using a simple, low-cost, and environmentally friendly emulsion polymerization approach, which produced a uniform coating and significantly improved the oil-absorption capacity. The structural formula, surface morphology and wettability of the modified sponges were characterized using Fourier transform infrared (FTIR) spectroscopy, scanning electron microscopy (SEM), and contact angle measurement techniques, respectively. The key parameters influencing the modification, including the amount of monomer, selection of the water/ethanol ratio and the concentration of the cross-linker divinylbenzene, were systematically optimized. After surface treatment, the water contact angle of the sponge increased significantly from about 85° to 154°, representing strong hydrophobicity. The modified sponges exhibited excellent selectivity, efficiently removing oils and organic liquids from oil/water and organic liquid/water systems, respectively, at saturation. They delivered high absorption capacities, ranging from 21 to 75 times their weight, while suppressing water uptake by approximately 94%. Furthermore, the materials achieved separation efficiencies exceeding 98.4% for trace oil removal and retained substantial absorption capacity even after 15 reuse cycles. These results demonstrate that a simple modification strategy can yield a low-cost, high-performance, and environmentally benign sponge, making it a highly promising candidate for oil spill remediation.

Received 12th February 2026
Accepted 3rd May 2026

DOI: 10.1039/d6ra01253a

rsc.li/rsc-advances

1. Introduction

Accidental releases from oil tankers and offshore drilling operations, along with natural events, such as earthquakes and hurricanes, have led to extensive marine oil contamination, posing serious environmental challenges on a global scale.[1–4] Especially, it has a negative impact on human health and seriously endangers marine life habitats. Oil spills occur frequently and incur substantial remediation costs, underscoring the urgent need for absorbent materials that are both economically viable and environmentally sustainable.[5,6]

A variety of materials, including absorbents and dispersing agents, can be utilized to achieve oil–water separation. Some examples are mineral goods,[7] chemical dispersants,[8] polymers,[9] textiles or fibers,[9,10] metallic meshes,[11] and carbon-based materials,[12] and they have been used for oil–water separation. However, several of these materials have drawbacks, such as poor water and oil separation efficiency, insufficient absorption, difficulty in manufacturing, recontamination, and lack of strength.[13,14] Porous materials have attracted considerable attention from scientists as effective candidates for oil-spill remediation. Their interconnected matrix architectures enable the efficient uptake and strong retention of oil, which can be subsequently recovered in a semi-solid form for convenient handling and reuse.[3,15–17]

Polyurethane (PU) sponge is a three-dimensional (3D), lightweight, low-density, open-cell porous material, making it a highly effective oil sorbent.[18,19] However, they are naturally amphiphilic and cannot separate an oil–water mixture on their own. On the other hand, superhydrophobic and superoleophilic materials may be perfect for cleaning up oil spills as they can selectively absorb large amounts of oil, do not react with solvents, and are easy to recycle.[12] Consequently, several investigations have concentrated on the hydrophobic modification of PU.[20–24] For example, Wang *et al.*[25] used dopamine to bind Fe_3O_4 nanoparticles to a PU skeleton and then added a fluorine-containing siloxane to make it water-repellent. It produced a magnetic, superhydrophobic PU material. Yang and his co-workers[14,26] demonstrated the modification of polyurethane (PU) using a polymer, lauryl methacrylate (PLMA), by dispersion polymerization. Xia *et al.*[27] modified the PU sponge with

[a]*Chemistry Discipline, Khulna University, Khulna-9208, Bangladesh. E-mail: mkhasan@ku.ac.bd*

[b]*Department of Chemistry, College of Science, Imam Mohammad Ibn Saud Islamic University (IMSIU), Riyadh 11623, Saudi Arabia*

reduced graphene oxide and the material showed very good oil absorption capacity. Despite notable progress in this field, the surface modification of porous materials still frequently depends on complex instrumentation or costly processing techniques. Certain modification strategies raise environmental concerns as they often involve the substantial use of toxic organic solvents, such as toluene and tetrahydrofuran, along with fluorinated chemicals employed to lower surface energy, which can limit their environmental compatibility and acceptance.[26,28–31] To address these challenges, there is a clear need to develop a simple, cost-effective, and environmentally sustainable approach for modifying sponge materials to enhance their oil–water separation performance.

In the present study, we report a simple, one-pot and two-step emulsion polymerization approach to create a super-hydrophobic PU sponge. A dual-layer coating of polystyrene (PSt) and polylauryl methacrylate (PLMA) is built up onto the PU surface in the first and second steps. The key factor of this process is that the LMA is highly hydrophobic and very difficult to deposit onto the PU surface by emulsion polymerization. So, initial coating with PSt makes the PU surface hydrophobic, which enhances the affinity of the LMA monomers, as well as the oligoradicals produced in water, to the PU surface. Besides, the water–ethanol mixture is employed as the dispersion medium during polymerization, which not only offers a low-cost and environmentally friendly alternative but also facilitates PLMA deposition onto the PU surface, providing a uniform superhydrophobic coating. As a result, the fabricated PU-PSt-PLMA sponge is very effective at absorbing and separating oil from water.

2. Experimental

2.1 Materials

The monomers, styrene (St, >98.0%) and lauryl methacrylate (LMA, >97.0%), were purchased from Tokyo Chemical Industry Co., Ltd, Japan, and passed through basic alumina columns to remove the inhibitors. The radical initiator, potassium persulfate (KPS, >98.0%), was obtained from Kanto Chemical Co., Ltd, Tokyo, Japan. Divinylbenzene (DVB) and polyvinyl alcohol (PVA) were received from Tokyo Chemical Industry Co., Ltd, Japan. Ethanol (99.5%) was purchased from Sigma-Aldrich (USA), and DI water was sourced from Ecotech Water BD (Dhaka, Bangladesh). The base PU sponge was received from Total Sponge Co., Ltd. The oils were obtained from a local market in Khulna, Bangladesh. The analytical reagent grade toluene, chloroform, hexane, and CCl_4 were obtained from Sinopharm Chemical Reagent Co., Ltd, Shanghai, China. These chemicals were of analytical grade and used without further purification.

2.2 Fabrication of the hydrophobic PU sponge

First, the PU sponges were cut into a square shape ($1 \times 1 \times 1$ cm^3) and ultrasonically cleaned with an ethanol-deionized water mixture for 30 min. The sponges were placed in an oven at 60 °C to dry completely. The modification reaction was carried out in a 100 mL three-necked reaction flask equipped with a thermometer and a reflux condenser. First, 0.036 g of KPS, 0.02 g of PVA, 0.5–1.5 g of styrene, and 0.003–0.007 g of DVB were added to the flask containing a different ratio of a water–ethanol mixture (30 g). After 20 minutes of stirring, the dried PU sponge (0.02 g) was totally immersed in the reactive solution for 3 h under stirring (550 rpm) at 70 °C. Second, 0.03 g of KPS and 0.1–0.3 g of LMA were slowly added to the flask for a 4 h reaction under the same conditions. After the reaction, the sponge was washed with a mixture of ethanol and deionized water three times, then dried at 60 °C under vacuum for 48 h, yielding a modified PU sponge named PU-PSt-PLMA sponge. The experimental scheme for the preparation of a super-hydrophobic PU sponge is shown in Fig. S1.

2.3 Absorption capacity test

The absorption performance of the PU-PSt-PLMA sponge was evaluated using various oils and organic solvents, including toluene, carbon tetrachloride, chloroform, kerosene, *n*-hexane, soybean oil, and diesel. All experiments were conducted at room temperature. For each sorption test, 50 mL of oil or organic solvent was placed in a 100 mL beaker, and the pre-weighed sponge was immersed in the oil. The sponge was gently removed using tweezers, drained of the excess liquid, and subsequently transferred to a pre-weighed container to measure the sponge's weight. Then, the oil absorption capacity was calculated using eqn (1) as follows:

$$\text{Oil sorption(g/g)} = \frac{(M_t - M_o)}{M_o}, \quad (1)$$

where M_0 and M_t represent the weight of the sponge before and after oil absorption, respectively. All measurements were repeated five times to ensure accuracy. The experiment on the capacity of water absorption was also performed similarly.

2.4 Separation efficiency test

The efficiency of oil–water separation was evaluated using a gravimetric method. First, a known amount of oil (1.2 g) was added to 220 mL of water to prepare the mixture. The dry sponge was weighed on an analytical balance to determine its initial weight (W_1). Then, the sponge was submerged in the mixture and allowed to absorb the oil until saturated. Afterward, it was carefully removed, and any surface liquid was gently wiped off with a filter paper without pressing. The sponge was immediately weighed again to record the final weight (W_2), and the amount of oil absorbed was calculated as $W_2 - W_1$. The remaining oil (N) was calculated from the mass balance as $N = N_0 - (W_2 - W_1)$. The separation performance was determined using eqn (2) for various oil–water systems, based on the change in oil mass before and after absorption from the mixture as follows:

$$S(\%) = \frac{N_0 - N}{N_0} \times 100, \quad (2)$$

where S (%) and N_0 represent the separation efficiency and initial oil weight prior to the absorption, respectively, and N indicates the remaining oil after the separation process. The

residual oil concentration in the treated water was also calculated as: $\text{ppm(mg/L)} = \frac{N}{V}$, where N represents the remaining oil (mg) after separation, and V indicates the volume of water (L) in the prepared mixture.

2.5 Reusability test

The reusability and mechanical stability of the modified PU sponge were examined over 15 successive absorption–release cycles. The retained oil was extracted by mechanically squeezing the sponge, eliminating the need for solvent evaporation. The sorption capacity for each reuse cycle (R) was determined to evaluate cyclic performance in accordance with eqn (3) as follows:

$$R(\text{g/g}) = \frac{S_1 - S_2}{S_2}, \quad (3)$$

where S_1 denotes the sponge weight after oil absorption, and S_2 represents the sponge weight after squeezing. This assessment effectively highlighted the capability to maintain the structural integrity, as well as absorption capacity, over multiple uses, showing its strong ability for practical uses and sustainability for oil–water separations.

2.6 Characterization and measurement

The successful coating of the sponge sorbent was verified through Fourier transform infrared (FTIR) spectroscopy (FT-720, HORIBA Ltd, Japan). Measurement was carried out over the range of 400–4000 cm^{-1} using 32 scans, and the spectral resolution was 4 cm^{-1}. The surface morphology of the sponges was investigated using scanning electron microscopy (SEM, JSM-7600FA, JEOL Ltd, Japan). Before analysis, the sponge sample was gold-coated on an aluminum stub prior to imaging to improve electrical conductivity. The wettability of the modified sponge was assessed by measuring the static water contact angle under ambient conditions using a Data Physics OCA 20 contact angle goniometer (Stuttgart, Germany). These characterizations provided detailed insight into the chemical and morphological properties of the modified sponges.

3. Results and discussion

3.1 Fabrication of superhydrophobic and superoleophilic PU sponges

Fig. 1 presents the schematic of the straightforward polymer modification strategy employed to functionalize the PU sponge through the incorporation of PSt and PLMA. This modification process was carried out through a two-step semicontinuous emulsion co-polymerization of styrene and LMA monomers, along with polyvinyl alcohol (PVA) as a steric stabilizer and divinylbenzene (DVB) as a cross-linker. The unmodified PU sponge exhibited amphiphilic features due to the combination of hydrocarbon chains (–CH_2– and –CH_3) and aromatic rings, joining with polar groups, such as urethane (–NH–CO–O–).[32] Furthermore, in the polyol segments, the residual hydroxyl groups (–OH) could contribute a hydrophilic character, and this amphiphilic nature hindered the direct adsorption of a hydrophobic LMA monomer. As a result, the polymerization onto PU surfaces became difficult. To overcome this challenge, the PU surface was initially modified with styrene, which is a moderately hydrophobic monomer, to improve compatibility with LMA. Moreover, the solvent ethanol was incorporated into the emulsion media to enhance the solubility of LMA and facilitate fruitful polymerization, resulting in a successful polymer coating.[33] In the 1st step of this process, the surface coating of the PU sponge with PSt during emulsion polymerization was most likely governed by a combination of interfacial polymer growth, physical anchoring, and possible chemical interactions. Upon the thermal decomposition of KPS, sulfate radicals initiated the polymerization of styrene, leading to the formation of PSt oligomers in the aqueous phase. In the presence of the porous PU substrate, monomer and oligomer species diffused into the sponge matrix, enabling the *in situ* nucleation and growth of PSt directly on the PU surface. This process facilitated strong mechanical interlocking within the interconnected pores of the sponge, resulting in a strong physical anchoring of PSt onto the sponge matrix.

Furthermore, both PSt and PU contain hydrophobic segments; PSt is highly hydrophobic due to its aromatic phenyl groups, and PU contains soft segments (polyol chains) that can exhibit a hydrophobic character. Thus, hydrophobic–hydrophobic interactions promoted the adhesion of the PSt particles onto the PU surface, enhancing coating stability. Weak van der Waals forces and possible π–π interactions between aromatic moieties (originating from styrene units and aromatic diisocyanate-derived PU structures) further stabilized the coating. The incorporation of divinylbenzene (DVB) as a crosslinker produced a rigid, three-dimensional PSt network, which could form a continuous or semi-continuous coating that was physically locked onto the PU surface. This crosslinking improved coating durability and resistance to detachment. In addition, limited radical-induced grafting may occur *via* hydrogen abstraction from PU chains by sulfate radicals, generating macroradicals that initiate the covalent attachment of PSt.[14] Hydrogen bonding interactions, particularly in the presence of a polyvinyl alcohol stabilizer, may also contribute as a secondary bridging force with the urethane groups (–NH–CO–O–) of PU.

In the second stage of the two-step emulsion polymerization process, the attachment of PLMA onto the pre-formed PSt-modified PU sponge was governed by a combination of seeded polymerization, interfacial diffusion, and cooperative intermolecular interactions. Following the initial deposition of a crosslinked PSt layer (*via* divinylbenzene), the PSt-coated PU acted as a hydrophobic seed substrate for subsequent polymer growth. Upon the thermal decomposition of KPS, sulfate radicals initiated the polymerization of LMA, which preferentially partitioned into the hydrophobic PSt domains rather than forming new particles in the aqueous phase. This resulted in a seeded emulsion polymerization mechanism, leading to the formation of a conformal PLMA layer over the PSt-coated framework. Simultaneously, LMA monomers diffused into the PSt matrix, allowing the growing PLMA chains to become

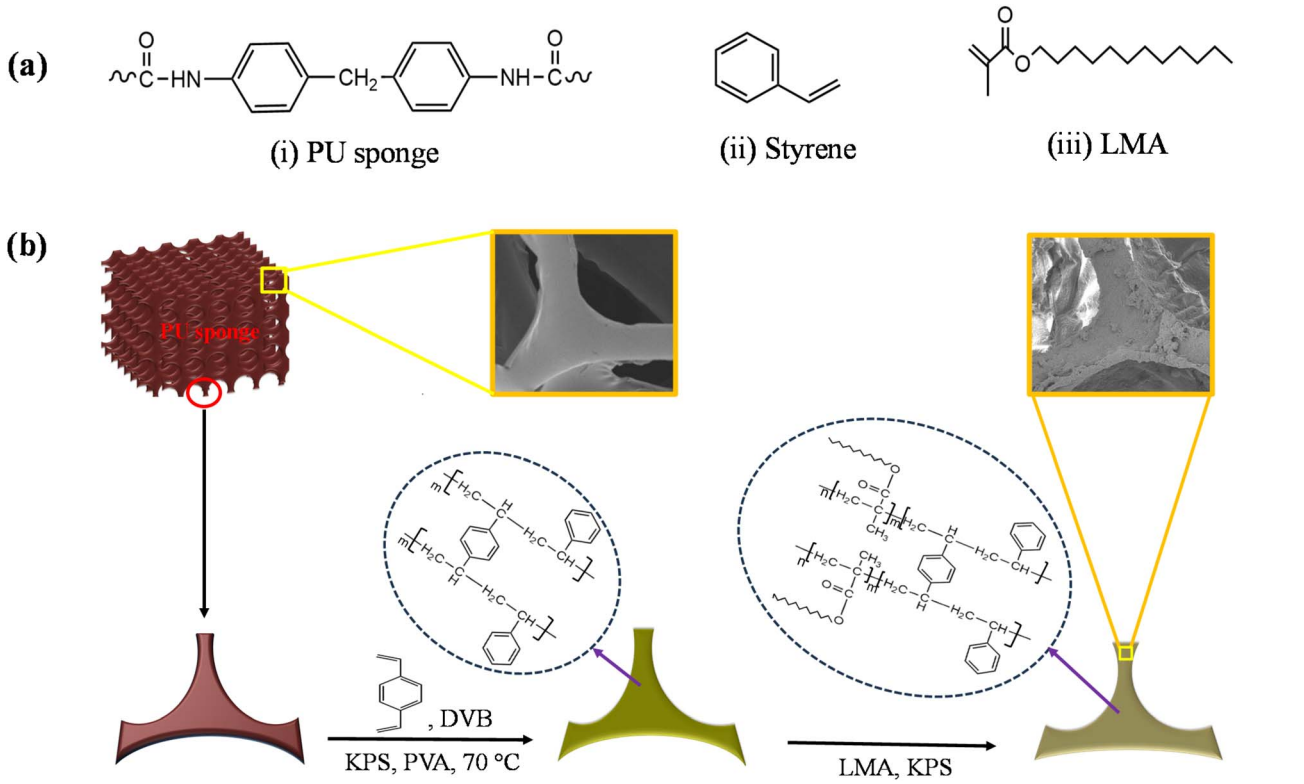

Fig. 1 (a) Chemical structures of (i) PU and the (ii) styrene and (iii) LMA monomers. (b) Plausible reaction scheme of the PSt and PLMA coatings on the PU sponge surface through emulsion polymerization.

physically entangled with the PSt chains, thereby generating strong topological anchoring. The long alkyl side chains of PLMA further promoted strong hydrophobic–hydrophobic interactions with the PSt surface, accompanied by enhanced van-der Waals interactions that improved chain packing and film cohesion. In addition, limited radical-induced grafting may occur *via* hydrogen abstraction from PSt chains, forming PSt macroradicals that initiate the covalent growth of PLMA, resulting in partial PS-g-PLMA linkages. The combined effects of interdiffusion and *in situ* polymer growth can also give rise to a semi-interpenetrating polymer network structure at the interface. Alongside these molecular–level interactions, the hierarchical porous structure of the PU sponge provided further mechanical interlocking, reinforcing the stability of the dual-layer coating. So, overall, the immobilization of PLMA onto the PSt-modified PU substrate was dominated by seeded polymer growth, chain entanglement, and hydrophobic interactions, with additional contributions from van-der Waals forces, partial covalent grafting, and interpenetrating network formation, ultimately leading to a robust, low-surface-energy coating with an enhanced hydrophobic performance.

3.2 Characterization of the modified PU sponge

3.2.1 FT-IR analysis. The FT-IR spectra of the (a) pristine PU sponge and modified (b) PU-PSt and (c) PU-PSt-PLMA sponges are observed in Fig. 2. The common peaks, including 3284 cm^{-1} (N–H stretching), 2970 cm^{-1} (–CH_2 stretching), 1710 cm^{-1} (C=O stretching of ester), 1640 cm^{-1} (C=O stretching of urea), 1540 cm^{-1} (N–H deformation), and 1090 cm^{-1} (C–O stretching), were present in both modified and unmodified sponges.[14] However, the peak intensities of the PU-PSt and PU-PSt-PLMA sponges at 2970, 1710, 1540, and 1090 cm^{-1} decreased

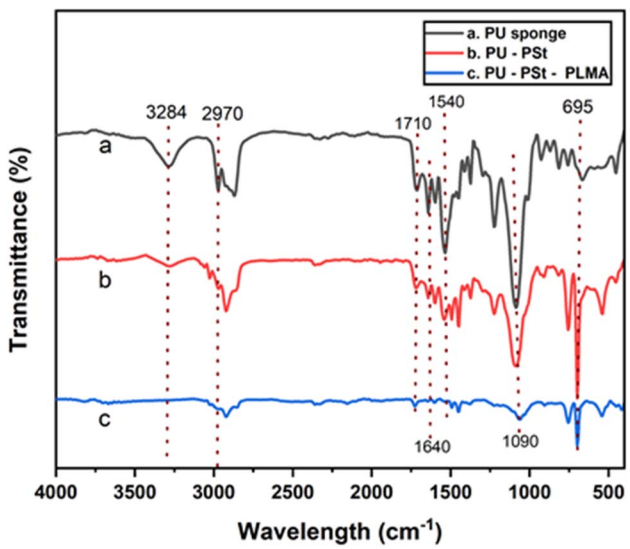

Fig. 2 FTIR spectra of the (a) pristine PU sponge and modified (b) PU-PSt and (c) PU-PSt-PLMA sponges.

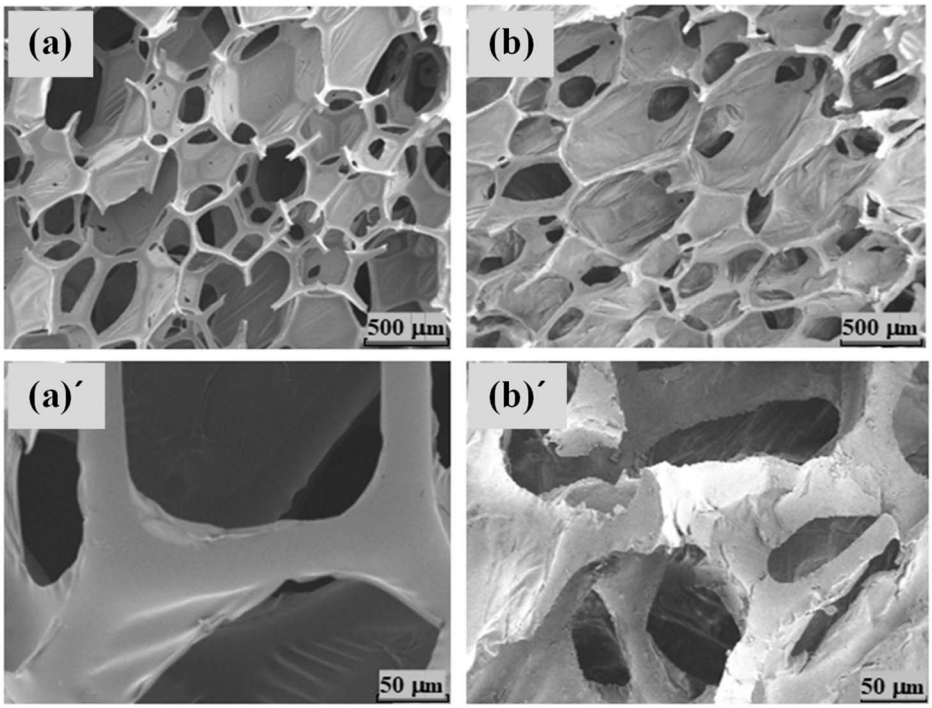

Fig. 3 SEM images of the unmodified PU sponge (a and a′) and modified PU-PSt-PLMA sponge (b and b′).

gradually compared with those of the pristine sponge due to fabricating a thin coating on the pristine sponge's surface.[34] The intensity of the pristine sponge's N–H stretching at 3284 cm^{-1} also decreased after styrene and LMA coating due to the PU surface coverage with PSt and PLMA through strong physical anchoring, along with partial covalent grafting by hydrogen elimination from the N–H bond. The C–H bond of styrene for the aromatic ring was visible with a prominent peak at 695 cm^{-1}, as shown in Fig. 2b,[35] but after PLMA attachment, the coating layer caused it to weaken (Fig. 2c). The results confirmed that the original PU sponge surface was coated with PSt-PLMA.

3.2.2 Surface morphology of the PU sponge. SEM images were used to study the surface morphologies of the PU sponge before and after (co) polymerization. Both the original and modified sponges held their distinctive three-dimensional porosity networks, as shown in Fig. 3, indicating that the pristine sponge's structure was not damaged during the modification process. The surface of the PU-PSt-PLMA sponge (Fig. 3a and a′) was significantly rougher than the surface of the pristine PU sponge (Fig. 3b and b′) due to the effective coating of polymeric layers onto the pristine sponge during polymerization. The increased surface roughness was a distinct indication that a hydrophobic coating had formed.[36] Overall, the findings revealed that the emulsion polymerization effectively produced a hydrophobic modified sponge while retaining its inherent three-dimensional structure, which was needed to maintain its flexibility and absorption capabilities in subsequent applications.

3.2.3 Hydrophobic and oleophilic properties. The hydrophilic and oleophilic properties of sponges were assessed by measuring their water contact angle (WCA) and oil contact angle (OCA). Water and soybean oil (as a model sample) droplets were placed on the sponge surface. Both water and oil were strongly attracted to the pristine sponge, as indicated by contact angles of 85° ± 1.2° for water (Fig. 4a) and 57° ± 0.8° for oil (Fig. 4b). When only styrene was used to modify the pristine PU sponge, the WCA of the PU-PSt sponge was increased to 135° ± 2.3°, as shown in Fig. 4c. It afforded a more hydrophobic surface than that of pristine because the coated polystyrene hydrocarbon chain reduced surface energy.[32,37] Though the PU-PSt sponge layer showed a high oil absorption rate with zero contact angle compared to the unmodified sponge (Fig. 4d), oil entered it very slowly. However, the surface of the PU-PSt sponge became significantly more hydrophobic after coating with additional poly(LMA) due to the long alkyl chains of LMA. The modified PU-PSt-PLMA showed a WCA of 154° ± 2.0° (Fig. 4e) and an OCA of 0° with good penetration (Fig. 4f), demonstrating the surface's total oleophilic nature.

The wettability behavior was clearly visible through the optical images displayed in Fig. 5. Super-hydrophobicity became apparent when a water droplet, colored with methylene blue for better visibility, was placed on the modified PU sponge surface, and it remained spherical. In contrast, the oil droplet exhibited great lipophilicity and was rapidly absorbed (Fig. 5a). The modified sponge floated more readily due to its increased hydrophobicity, but the unmodified sponge partially sank when submerged in water (Fig. 5b). However, when both

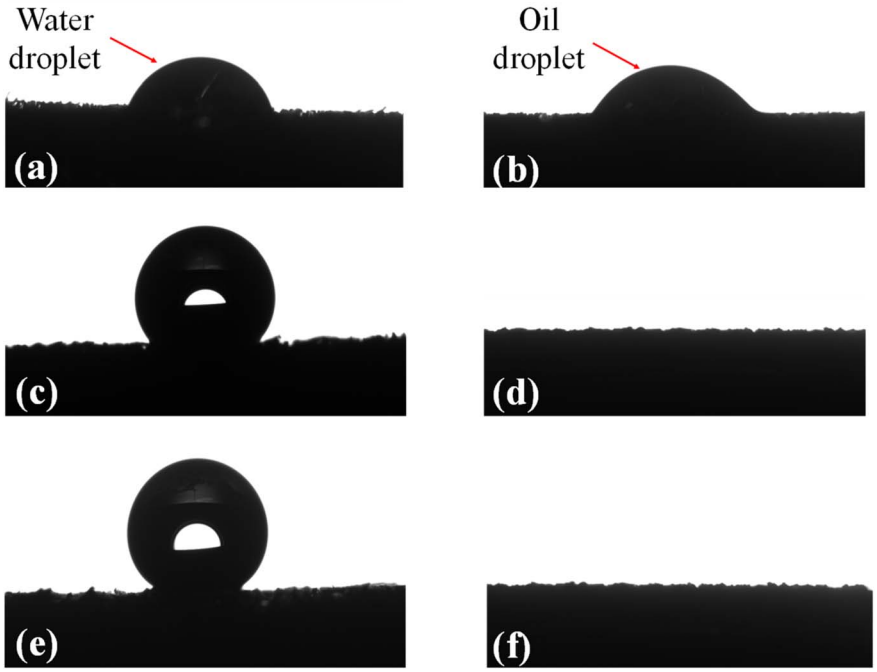

Fig. 4 Contact angle assessment for the sponges. Images of (a) a water droplet and (b) an oil droplet on the pristine sponge. Images of (c) a water droplet and (d) an oil droplet on the PU-PSt sponge. Images of (e) a water droplet and (f) an oil droplet on the PU-PSt-PLMA sponge.

sponges were submerged in oil, the unmodified sponge remained floating, but the modified sponge totally sank, indicating that it could potentially absorb oil (Fig. 5c). These results concluded that the modified sponge (PU-PSt-PLMA) had a superhydrophobic and super oleophilic nature, and oil absorption was very selective in terms of wettability.

3.3 Influence of the reaction recipes on WCA

3.3.1 Effect of the styrene content. Table S1 and Fig. 6a demonstrate how varying the styrene amount (0.50 to 1.50 g) influences the WCA. As the styrene level increased initially, the WCA also increased, reaching the maximum value of 150° ± 2.5° at 1.0 g of styrene. This result could be attributed to the surface coating procedure, which enabled this enhancement by forming a thin polystyrene (PSt) layer on the PU surface. By adding the phenyl hydrophobic ($-C_6H_5$) groups and roughening the surface, the PSt coating reduced surface energy and increased the composite's hydrophobicity. However, the WCA decreased when the styrene content exceeded 1.0 g. The decrease was probably because of too much polymerization, which made the PSt layer relatively thick and smooth,

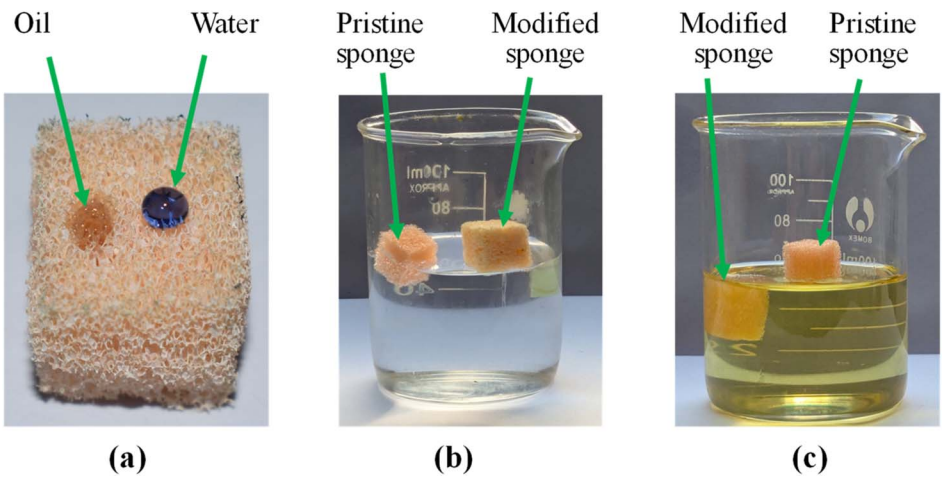

Fig. 5 Hydrophilic and lipophilic photographs of the modified sponge. (a) Photograph of an oil droplet and a water droplet on the PU-PSt-PLMA sponge. (b) Photograph of the immersion process of the pristine and modified sponges in water. (c) Photograph of the immersion process of the modified and pristine sponges in soybean oil.

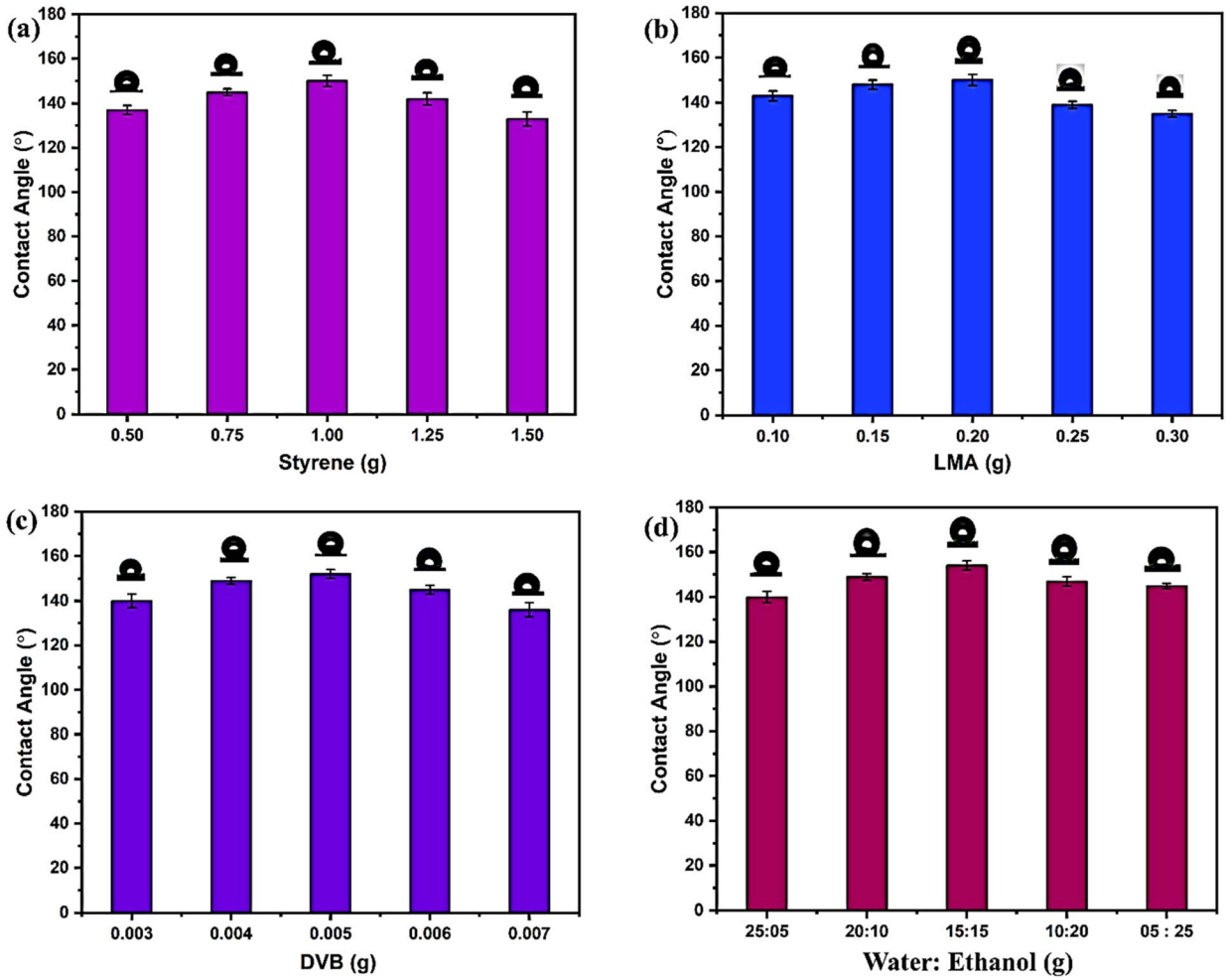

Fig. 6 Effect of the reaction conditions on the modification process of the water contact angle (WCA). (a) Styrene [reaction conditions: in the 1st step, DVB = 0.004 g, LMA = 0.2 g, H_2O = 20 g, ethanol = 10 g, PVA = 0.02 g and KPS = 0.036. In the 2nd step, KPS = 0.03 g. Polymerization temperature = 70 °C]. (b) LMA [reaction conditions: in the 1st step, DVB = 0.004 g, styrene = 1.0 g, H_2O = 20 g, ethanol = 10 g, PVA = 0.02 g and KPS = 0.036. In the 2nd step, KPS = 0.03 g. Polymerization temperature = 70 °C]. (c) DVB [reaction conditions: in the 1st step, styrene = 1.0 g, LMA = 0.2 g, H_2O = 20 g, ethanol = 10 g, PVA = 0.02 g and KPS = 0.036. In the 2nd step, KPS = 0.03 g. Polymerization temperature = 70 °C]. (d) Ethanol [reaction conditions: in the 1st step, DVB = 0.005 g, styrene = 1.0 g, LMA = 0.2 g, PVA = 0.02 g and KPS = 0.036. In the 2nd step, KPS = 0.03 g. Polymerization temperature = 70 °C].

subsequently making the surface less rough and less hydrophobic, as described by the Wenzel and Cassie–Baxter wetting models.[38,39] Additionally, excessive polymer deposition may block the PU sponge's porous structure, reducing air-trapping capacity. In fact, the 3D porous network of PU made it more hydrophobic by keeping an air–solid composite interface. When pores are blocked, the material can change from the Cassie–Baxter (composite) state to the Wenzel (fully wetted) state. Because of this modification, air has a hard time becoming trapped, lowering the WCA.[40]

3.3.2 Effect of the amount of LMA. The effect of the LMA content on WCA of the modified PU sponge was carefully studied under constant polymerization conditions, and the data are listed in Table S2, and the results are represented in Fig. 6b. The contact angle values showed a clear relationship with the dosage of LMA added to the system. As the monomer content increased from 0.1 to 0.2 g, the diffusion of the LMA molecules into the PU network improved, facilitating polymer deposition and yielding a maximum WCA of 150° ± 2.5°. This enhancement resulted from the inclusion of long hydrophobic alkyl chains from LMA, which reduced surface energy and increased water repellency. However, the further addition of LMA beyond 0.2 g led to a decrease in WCA to 135° ± 0.5°. The high monomer concentration promoted homopolymer formation and gelation, which blocked active sites and restricted further deposition onto the PU framework, decreasing the surface hydrophobicity.[26,41]

3.3.3 Effect of DVB amount. For polyurethane surface stability, a cross-linked network structure is essential. In the absence of sufficient cross-linking to maintain their structural integrity, even polymers with strong anchoring can disintegrate in solvents. The accompanying data are included in Table S3,

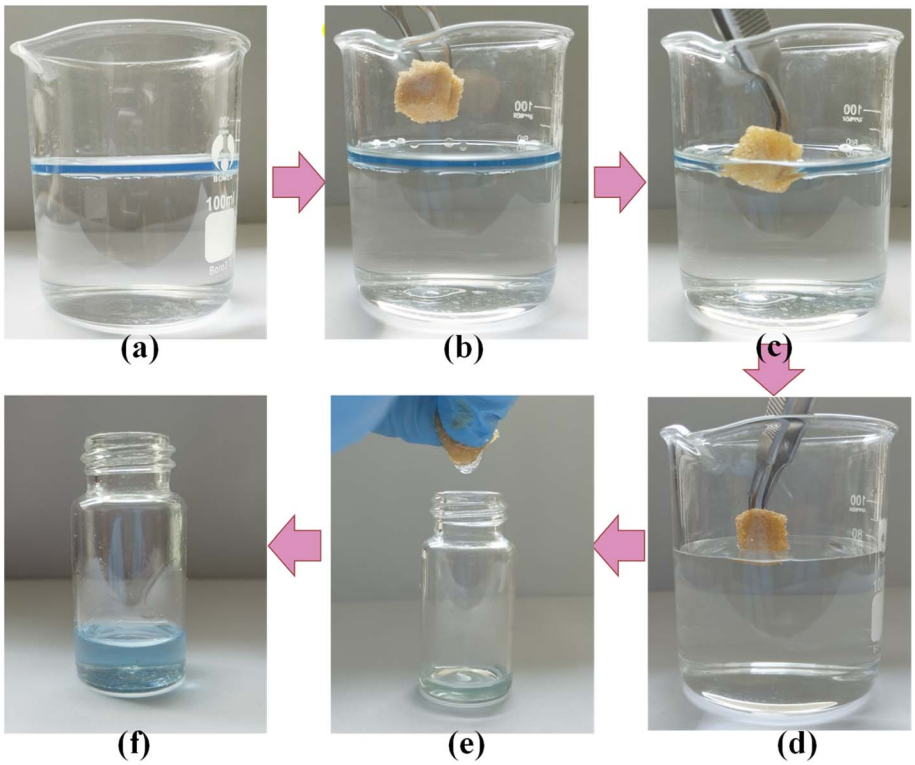

Fig. 7 Photographs (a–f) show the selective extraction of kerosene from the kerosene-water mixture using the PU-PSt-PLMA sponge.

and Fig. 6c illustrates how the WCA of the modified PU sponge is affected by DVB content. The WCA increased from 140° ± 3.0° to 152° ± 1.2° as the DVB concentration increased from 0.003 g to 0.005 g, indicating that the surface became more hydrophobic. This enhancement was achieved by creating a well-cross-linked hydrophobic network that stabilized the coated polymer layer and roughened the surface. Effective cross-linking between styrene and lauryl methacrylate chains produced a thick, persistent hydrophobic layer and reduced the exposure of polar groups (–OH, –COOH, and –NH) at moderate DVB levels.[42,43] However, WCA decreased with the increase in DVB above 0.005 g, reaching a minimum of 136° ± 3.2° at 0.007 g. Excessive DVB leads to an excessively compact, inflexible structure, hindering the ability of molecules to rearrange and exposing hydrophobic alkyl chains.[44] Moreover, too much cross-linking can cause surface coalescence or the collapse of micro/nano-scale roughness, which makes the surface smoother and less hydrophobic.[45,46]

3.3.4 Effect of the ethanol content. Lauryl methacrylate (LMA) has a low tendency for emulsion polymerization in a water medium due to its high hydrophobicity. Adding a cosolvent, such as ethanol, is essential for effective polymerization, as it reduces the polarity and surface tension of the aqueous phase, thereby facilitating the dispersion of hydrophobic monomers.[33] This study employed a water–ethanol mixed medium with varied ratios to investigate the influence of ethanol concentration on the WCA, as shown in Table S4 and Fig. 6d. A water–ethanol ratio of 15 : 15 was a modest level of ethanol, which yielded the best WCA of 154° ± 2°. At this scale, ethanol enhanced the miscibility of styrene, LMA, and DVB with the continuous phase. This allowed a more uniform placement of hydrophobic polymers onto the PU surface, making it relatively rough. However, the WCA decreased at high ethanol concentrations. Excess ethanol made the medium too non-polar, leading to phase splitting, particle adhesion, and irregular coating on the PU surface. As a result, the hydrophobic layer became uneven, revealing the underlying hydrophilic matrix.[47,48] Furthermore, high concentrations of ethanol may lead to the expansion or increased plasticity of the PU structure, potentially resulting in the re-emergence of polar urethane or urea groups on the surface after drying, which reduces the overall WCA.

3.4 Selective oil/water separation

The selective absorption of the modified sponges (Table S4; S-18) was examined for light oil, kerosene, and a heavy organic solvent, dichloromethane. In the kerosene-water system, there was a distinct phase separation, with kerosene at the top and water at the bottom (Fig. 7a). Upon the placement of the modified sponge (Fig. 7b), it rapidly and selectively absorbed kerosene while repelling water, as seen in Fig. 7c and d. This selective sorption characteristic arose from modifying the sponge's surface to make it highly hydrophobic and oleophilic. It suggested that the modified sponges exhibited improved separation efficiency and captured the oil effectively. Furthermore, the retained oil (kerosene) could be easily extracted by simple mechanical squeezing, as presented in Fig. 7e and f,

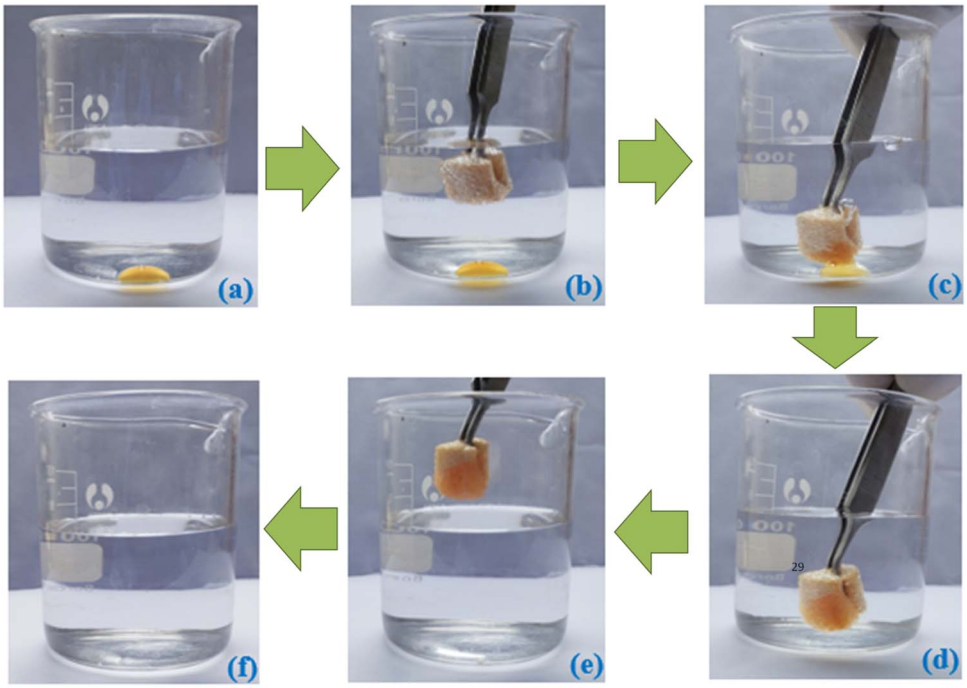

Fig. 8 Photographs (a–f) depicting the separation process of dichloromethane (organic solvent) from beneath the water surface using the PU-PSt-PLMA sponge.

demonstrating its flexible nature and potential for repeated uses.

Moreover, Fig. 8 demonstrates that the treated sponge efficiently removes heavy organic contaminants from beneath the water surface. In this experiment, dichloromethane (a heavy organic liquid), which was colored with aniline, accumulated on the bottom of the container due to its high density (Fig. 8a). Upon submerging the modified sponge into the mixture, a distinct silver sheen appeared, which was attributed to the trapped air layer that maintained a dry surface and repelled water (Fig. 8b).[49] This unique character empowered the sponge to preferentially absorb the dichloromethane that is immiscible with water (Fig. 8c and d).

The recovered dichloromethane was completely free from water (Fig. 8e), highlighting the strong separation efficiency of the modified sponge. This finding demonstrated that the engineered sponge possessed excellent hydrophobic and oleophilic capabilities. Hence, the material is a promising candidate for environmental remediation, especially for separating the oil–water mixtures and removing organic pollutants.

3.5 Mass absorption capacity

The absorption capacity of the modified sponge toward a variety of oils and organic solvents, including toluene, diesel, chloroform, carbon tetrachloride, kerosene, soybean oil and *n*-hexene, was quantitatively measured following eqn (1). Considerable differences were noticed in the absorption behaviors of the modified sponges (Table S4: S-17, S-18, S-19, and S-20), which are presented in Fig. 9. Among these modified samples, S-18 showed the highest sorption capacity, retaining approximately 21–75 times its weight at the saturation stage. The highest absorption was observed at 75 g g^{-1} for chloroform, whereas diesel exhibited the lowest value at 21 g g^{-1}. The enhanced absorption of chloroform in the PSt/PLMA-modified PU sponge could be attributed to a combination of favorable physicochemical interactions and efficient transport behavior between the solvent and the polymer coating. Although the coating composed of PSt and PLMA was predominantly hydrophobic, it contained aromatic rings and ester functionalities that could interact with moderately polar and highly polarizable solvents. Chloroform possessed slight polarity and high polarizability, enabling strong van der Waals and weak dipole-induced dipole interactions with both components of the coating.[50] These interactions enhanced solvent affinity and uptake compared to highly nonpolar solvents, such as *n*-hexane or kerosene, which exhibited limited interaction with the polymer matrix.

In addition, chloroform is an effective swelling solvent for polystyrene domains. It could partially plasticize the PSt segments, increasing the free volume within the coating and facilitating deep penetration into the sponge's porous structure. While toluene also exhibited swelling capability toward polystyrene, its overall interaction in this composite system was comparatively less efficient due to differences in polarity and diffusion dynamics.[50,51] Transport properties further contributed to the observed behavior. Chloroform has low viscosity, which promotes rapid capillary-driven infiltration into the interconnected porous network. In contrast, more viscous liquids, such as diesel, soybean oil, and kerosene, diffused more slowly, resulting in reduced absorption within the same time frame.[52] Moreover, chloroform's relatively high density

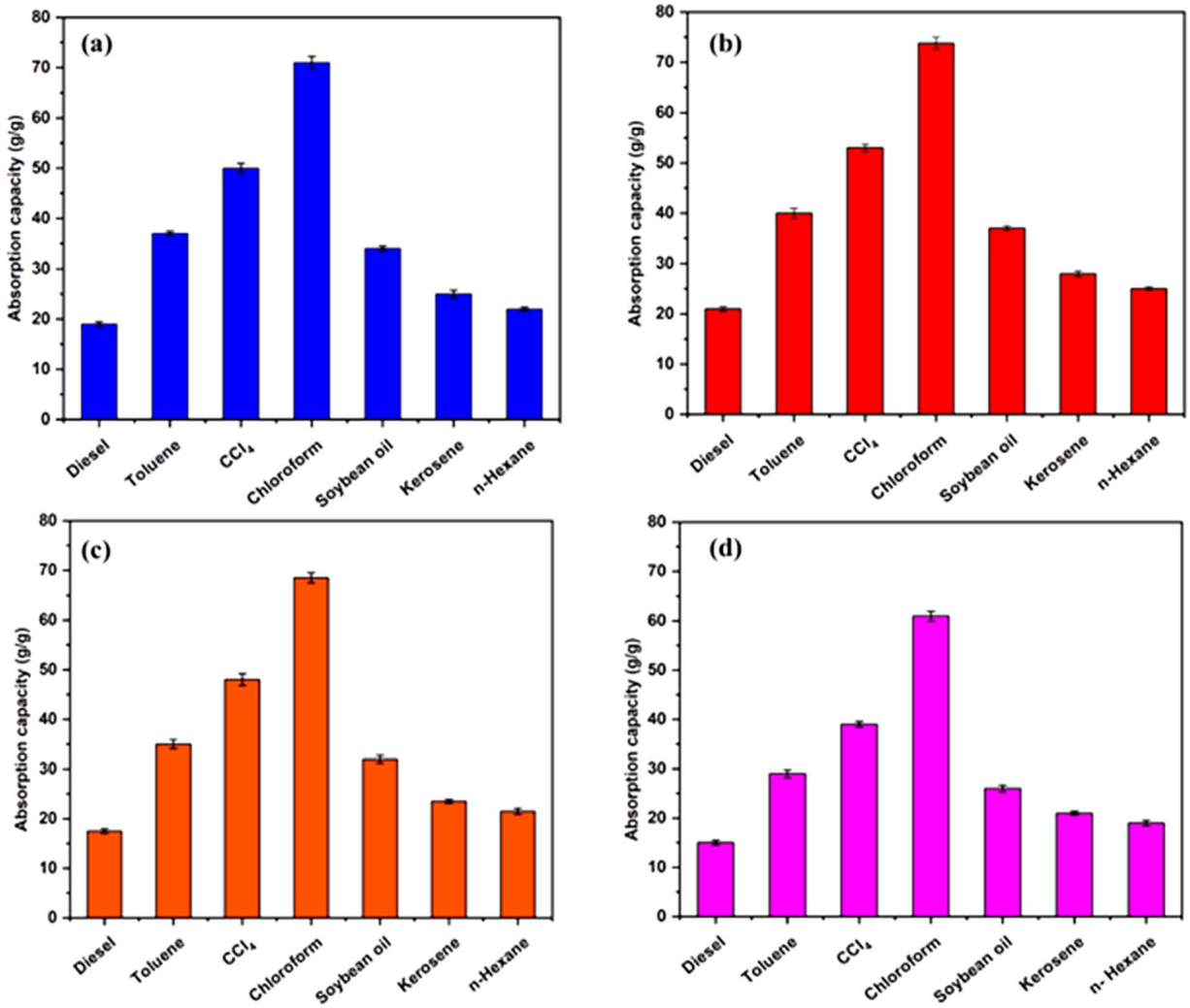

Fig. 9 Absorption capacity of the modified sponges, (a) S-17, (b) S-18, (c) S-19, and (d) S-20, for different kinds of oil and organic liquid samples, including diesel, toluene, CCl_4, chloroform, soybean oil, kerosene and *n*-hexane.

(1.49 g cm^{-3}) contributed to high gravimetric uptake values (g g^{-1}), as equivalent pore filling led to greater measured mass. Finally, its small molecular size facilitated fast diffusion into the micro- and meso-pores of the modified sponge, whereas bulky hydrocarbon mixtures experienced steric hindrance, further limiting their uptake.[53]

The water absorption capacity of the pristine PU sponge was 7.7 ± 0.20 g g^{-1}, but following surface modification, it considerably dropped to 0.5 ± 0.08 g g^{-1} (Fig. 10). This significant decrease attests to the modified sponge's increased hydrophobicity. The PU-PSt-PLMA sponge achieved water contact angles and oil/organic solvent absorption capacities comparable to those of other reported high-performance PU-based sorbents, as summarized in Table 1.

3.6 Separation efficiency in a water–oil system

The separation effectiveness of the modified sponge (Table S4; S-18) for different oil–water mixtures was assessed using eqn (2). Mixtures of toluene/water, carbon tetrachloride/water, chloroform/water, kerosene/water, *n*-hexane/water, soybean oil/water, and diesel/water were successfully separated. Fig. 11 illustrates that the modified PU sponge attained a separation efficiency of 98.4%, while the residual oil concentration in the treated water remained under 90 ppm. The high efficiency was sustained in several oil–water systems, indicating the sponge's good selectivity and flexibility. These outstanding findings highlighted the excellent absorption performance of the modified sponge to separate oil from water, which indicated its high potential as a usable material for halting environmental pollution, particularly in recovering, as well as cleaning, spilled oil and for wastewater treatment.

3.7 Reusability

The reusability of the modified sponge is a critical consideration to assess the practical applicability. The reuse performance of the sponge sample (Table S4; S-18) was investigated through several absorption/desorption experiment cycles with the help of eqn (3). Owing to its remarkable elasticity and

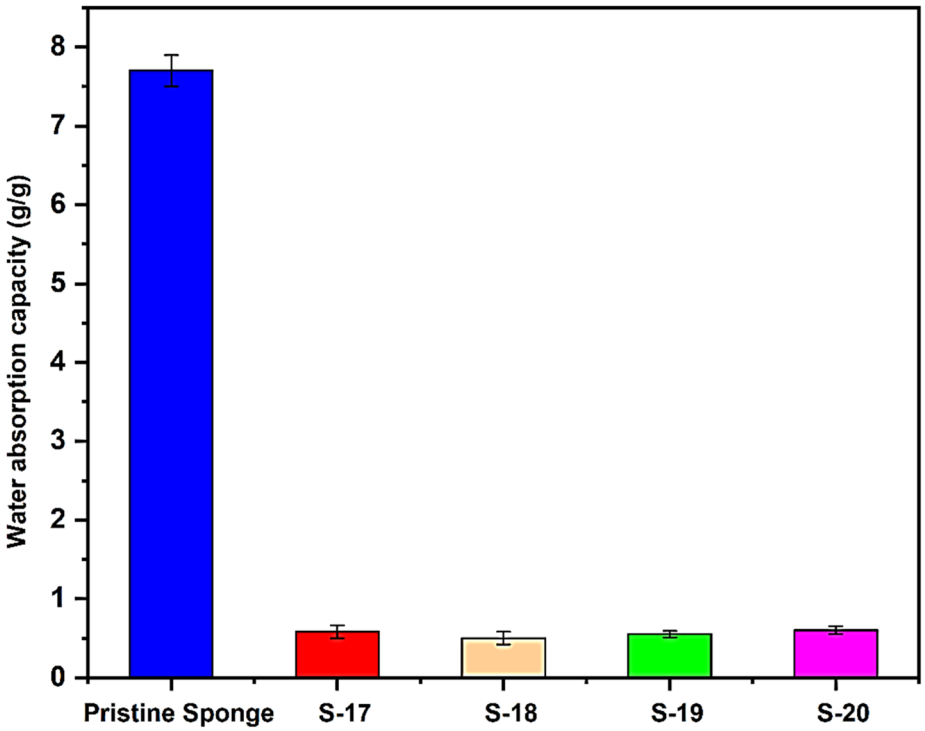

Fig. 10 Water absorption comparison test of the pristine sponge with the modified sponges S-17, S-18, S-19, and S-20.

Table 1 Comparison of the absorption capacities and water contact angles of various modified sponges

Modified PU sponge	Modification method	Oils/organic solvents	Absorption capacity (g g^{-1})	WCA	Ref.
PDMS-PU	Dip coating	Toluene, hexane, silicon oil, gasoline, soybean oil, chloroform, and xylene	21–48	148°	37
Fe_3O_4-PU sponge	Dip coating	Peanut oil, silicon oil, and lubricating oil	20–21.7	—	54
GO-PU sponge	Dip coating	Tetrachloromethane, *n*-hexane, dichloromethane, sesame oil, xylene, and kerosene	16–35	151°	55
SiO_2-PU sponge	Dip coating	Kerosene, petroleum ether, chloroform, *n*-hexane, and *n*-heptane	33–55.8	150°	56
SiO_2-PDA-PU sponge	Dip coating/ polymerization	*n*-Hexane, crude oil, toluene, and chloroform	18–46.8	154°	57
NDs-PU sponge	Dip coating	Chloroform, diesel, pump oil, gasoline, ethanol, toluene, hexadecane, and hexane	15–60	160°	58
FAS-17/Fe_3O_4-PU sponge	Dip coating/ polymerization	*n*-Hexane, solvent naphtha, petroleum ether, benzene, gasoline, THF, kerosene, and lubricating oil	10–35	152°	59
Polymer brush/ PU sponge	Polymerization	Crude oil, peanut oil, toluene, methanol, acetone, chloroform, *n*-hexane, and petroleum ether	17–40	151°	60
PPy-PA PU sponge	Polymerization	Carbon tetrachloride, *n*-decane, *n*-heptane, and sunflower oil	22–62	140°	61
NMP/graphene PU sponge	Polymerization	Hexane, crude oil, octane, and engine oil	40–80	151°	62
LMA-g-PU sponge	Polymerization	Benzene, toluene, and carbon tetrachloride	40–50.4	—	14
St/LMA-PU sponge	Polymerization	Diesel, toluene, carbon tetrachloride, chloroform, soybean oil, kerosene, and *n*-hexane	21–75	154° ± 2°	This work

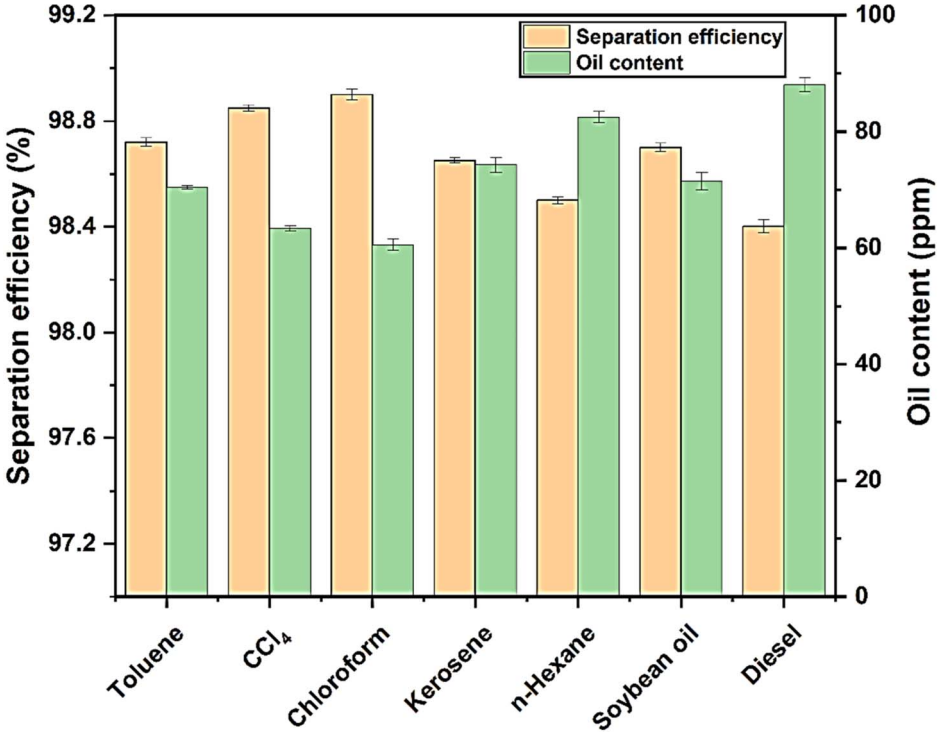

Fig. 11 Oil and organic-liquid separation performance of the modified sponge S-18 assessed in various oil/water systems.

structural durability, the absorption capacity remained largely unchanged for various oils and organic liquids throughout the 15 consecutive absorption cycles and squeezing. The performance results are displayed in Fig. 12. These durable features indicated that the fabricated sponges were well-suited to repeated applications in practical uses. In addition, the modified sponge effectively preserved its structural integrity despite repeated compression, maintaining more than 90% of its initial height over 10 cycles, and the results are exhibited in Fig. 13. So, this experiment further reflected the strong flexibility and

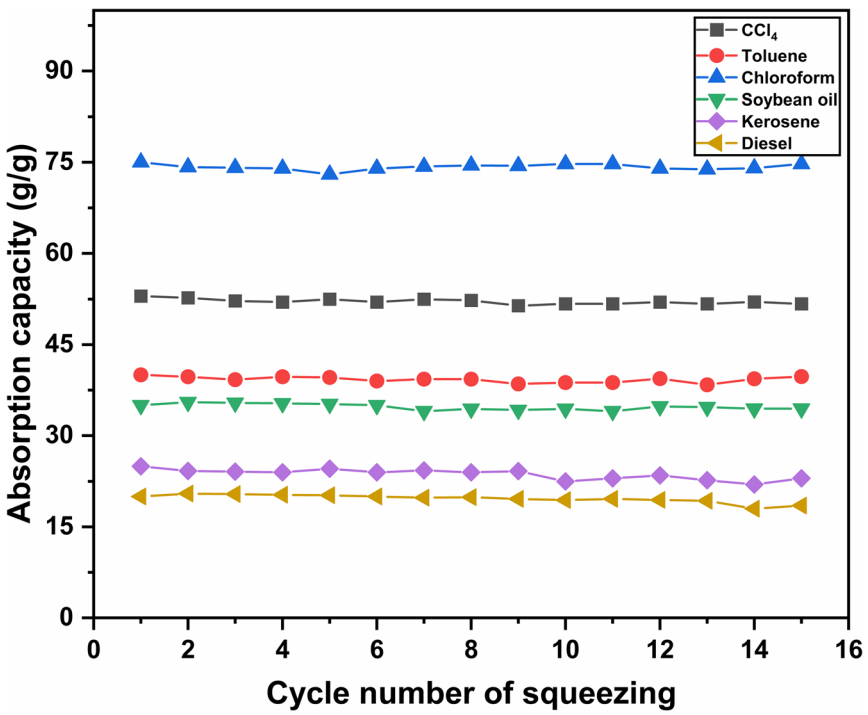

Fig. 12 Reusability test of the modified sponge S-18 for 15 consecutive absorption cycles and squeezing.

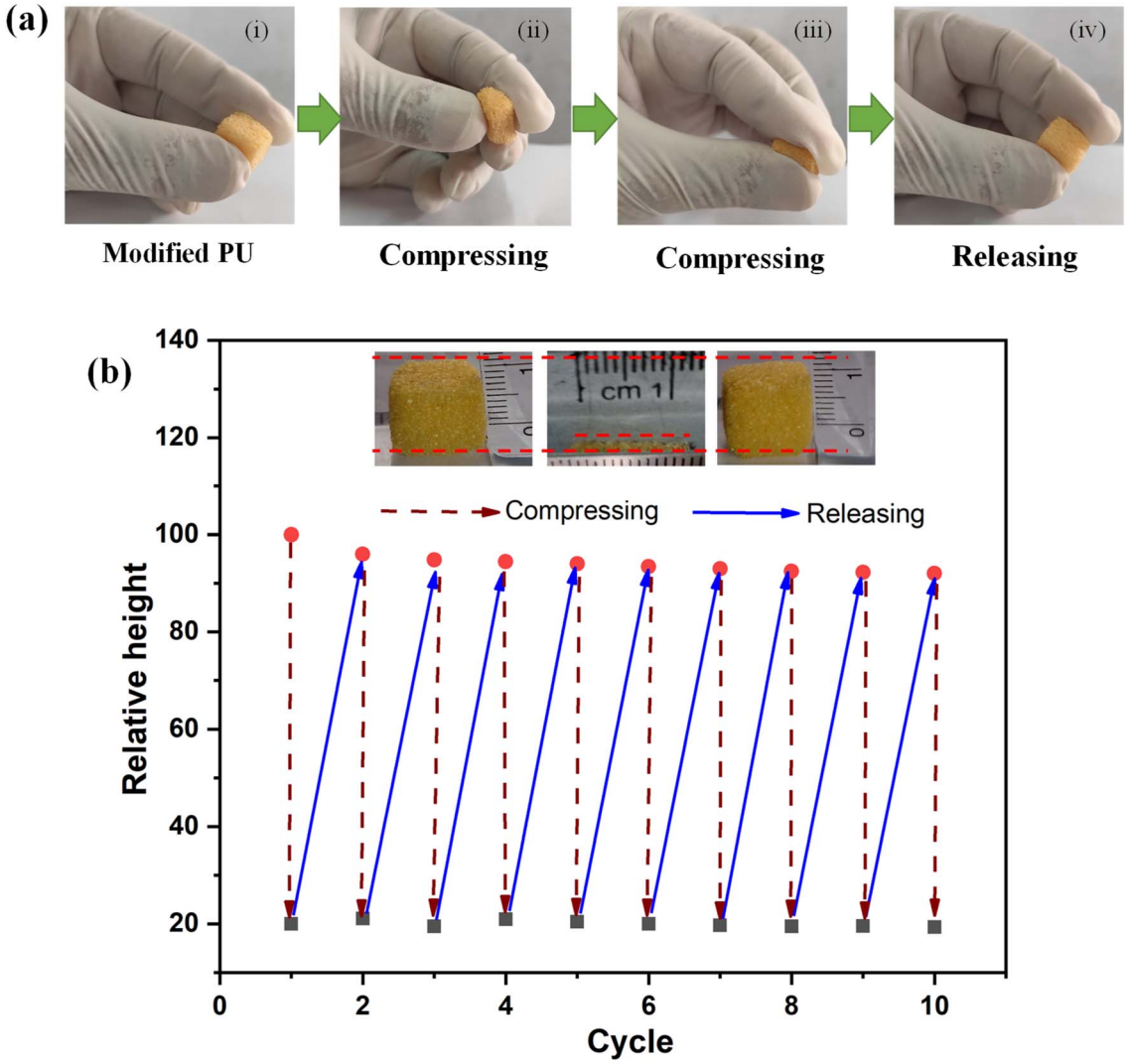

Fig. 13 Exhibition of the elastic behavior of the fabricated sponge sample (S-18). (a) Photographs (i–iv) showing the sponge retaining its intrinsic flexibility in the PU framework. (b) Changes in the height of the sponge over 10 consecutive compression cycles, showing its ability to recover after repeated deformation.

mechanical durability, with pronounced oil affinity and water repellency.

4. Conclusions

The polyurethane sponge was successfully modified *via* a facile, cost-effective, and environmentally benign emulsion polymerization approach using styrene and a highly hydrophobic monomer, LMA. The resulting PU-PSt-PLMA composite foam exhibited outstanding water repellency, excellent mechanical flexibility, and robust long-term durability while preserving its intrinsic hierarchical porous structure. Owing to these advantageous characteristics, the modified sponge demonstrated exceptional selectivity and efficiency in capturing a wide spectrum of oils and organic solvents, particularly from oil–water systems, underscoring its strong potential for mitigating marine and aquatic pollution. Notably, the engineered sponge delivered a high absorption capacity ranging from approximately 21 to 75 times its weight, coupled with an impressive separation efficiency of up to 98%. Furthermore, it maintained consistent performance over multiple reuse cycles, highlighting its excellent reusability. Collectively, these attributes position the modified PU sponge as a highly promising material for the efficient and sustainable removal of oils and organic contaminants from water environments.

Author contributions

Md. Ariful Islam Setu: validation, investigation, methodology, formal analysis, software, and writing-original draft. Md. Suzon Ahmed: writing-review and editing. Md. Kamrul Hasan: conceptualization, visualization, methodology, software, writing-review and editing, and dupervision. Ahmed B. M. Ibrahim: writing-review and editing. Muhammad Sarwar Hossain: writing-review and editing. Md. Rezaul Haque: visualization and writing-review and editing.

Conflicts of interest

The authors declare that they have no known financial or personal conflicts of interest.

Data availability

The data supporting the findings of this study can be obtained from the corresponding author upon request. Due to privacy concerns and other restrictions, the data are not publicly accessible.

Supplementary information (SI) is available. See DOI: https://doi.org/10.1039/d6ra01253a.

Acknowledgements

The authors are grateful to the Chemistry Discipline, Khulna University, Khulna-9208, for providing the necessary laboratory facilities. The authors are also very grateful to the Research and Innovation Centre at Khulna University, Khulna-9208, Bangladesh, for the financial support (Grant ID : RICKU/04/(166)2000–324).

References

1 K. Bensadok, M. Belkacem and G. Nezzal, *Desalination*, 2007, **206**, 440–448.
2 F. Ding and M. Gao, *Adv. Colloid Interface Sci.*, 2021, **289**, 102377.
3 Y.-Q. Zhang, Q.-D. An, Z.-Y. Xiao, K.-R. Zhu, X.-L. Dong and S.-R. Zhai, *Int. J. Biol. Macromol.*, 2023, **253**, 127368.
4 Y.-Q. Zhang, Y.-H. Jiang, Y.-N. Qin, Q.-D. An, L.-P. Xiao, Z.-H. Wang, Z.-Y. Xiao and S.-R. Zhai, *Colloids Surf., A*, 2022, **643**, 128790.
5 T. Neuparth, S. M. Moreira, M. M. Santos and M. A. Reis-Henriques, *Mar. Pollut. Bull.*, 2012, **64**, 1085–1095.
6 I. B. Ivshina, M. S. Kuyukina, A. V. Krivoruchko, A. A. Elkin, S. O. Makarov, C. J. Cunningham, T. A. Peshkur, R. M. Atlas and J. C. Philp, *Environ. Sci.:Processes Impacts*, 2015, **17**, 1201–1219.
7 M. O. Adebajo, R. L. Frost, J. T. Kloprogge, O. Carmody and S. Kokot, *J. Porous Mater.*, 2003, **10**, 159–170.
8 S. Kleindienst, J. H. Paul and S. B. Joye, *Nat. Rev. Microbiol.*, 2015, **13**, 388–396.
9 J. Ge, H. Y. Zhao, H. W. Zhu, J. Huang, L. A. Shi and S. H. Yu, *Adv. Mater.*, 2016, **28**, 10459–10490.
10 M. Seddighi and S. M. Hejazi, *Mar. Pollut. Bull.*, 2015, **96**, 286–293.
11 B. Wang, W. Liang, Z. Guo and W. Liu, *Chem. Soc. Rev.*, 2015, **44**, 336–361.
12 S. Gupta and N.-H. Tai, *J. Mater. Chem. A*, 2016, **4**, 1550–1565.
13 Q. Ma, H. Cheng, A. G. Fane, R. Wang and H. Zhang, *Small*, 2016, **12**, 2186–2202.
14 H. Li, L. Liu and F. Yang, *Mar. Pollut. Bull.*, 2012, **64**, 1648–1653.
15 N. Zhang, Y. Qi, Y. Zhang, J. Luo, P. Cui and W. Jiang, *Ind. Eng. Chem. Res.*, 2020, **59**, 14546–14568.
16 H. Huang, X. Li, C. Zhao, L. Zhu, Y. Li, Y. Wu and Z. Li, *J. Mater. Sci.*, 2022, **57**, 336–350.
17 W. Zhang, Z. Shi, F. Zhang, X. Liu, J. Jin and L. Jiang, *Adv. Mater.*, 2013, **25**, 2071–2076.
18 G. Harikrishnan, T. U. Patro and D. V. Khakhar, *Ind. Eng. Chem. Res.*, 2006, **45**, 7126–7134.
19 H. Huang, C. Zhao, J. Li, J. Cheng, D. Xiang, J. Wei, Y. Yang, Z. Li, Y. Li, M. Qin and Y. Wu, *Colloids Surf., A*, 2023, **658**, 130710.
20 M. Peng, Y. Zhu, H. Li, K. He, G. Zeng, A. Chen, Z. Huang, T. Huang, L. Yuan and G. Chen, *Chem. Eng. J.*, 2019, **373**, 213–226.
21 T. Yu, F. Halouane, D. Mathias, A. Barras, Z. Wang, A. Lv, S. Lu, W. Xu, D. Meziane, N. Tiercelin, S. Szunerits and R. Boukherroub, *Chem. Eng. J.*, 2020, **384**, 123339.
22 S. Ye, B. Wang, Z. Pu, T. Liu, Y. Feng, W. Han, C. Liu and C. Shen, *Sep. Purif. Technol.*, 2021, **266**, 118553.
23 Z.-T. Li, B. Lin, L.-W. Jiang, E.-C. Lin, J. Chen, S.-J. Zhang, Y.-W. Tang, F.-A. He and D.-H. Li, *Appl. Surf. Sci.*, 2018, **427**, 56–64.
24 L. Liang, Y. Dong, Y. Liu and X. Meng, *Polymers*, 2019, **11**, 2072.
25 Y. Shi, B. Wang, S. Ye, Y. Zhang, B. Wang, Y. Feng, W. Han, C. Liu and C. Shen, *Appl. Surf. Sci.*, 2021, **535**, 147690.
26 H. Li, L. Liu and F. Yang, *Procedia Environ. Sci.*, 2013, **18**, 528–533.
27 C. Xia, Y. Li, T. Fei and W. Gong, *Chem. Eng. J.*, 2018, **345**, 648–658.
28 S. Liu, Q. Zhang, L. Fan, R. Wang, M. Yang and Y. Zhou, *Ind. Eng. Chem. Res.*, 2020, **59**, 11713–11722.
29 U. Azhar, C. Huyan, X. Wan, C. Zong, A. Xu, J. Liu, J. Ma, S. Zhang and B. Geng, *Arab. J. Chem.*, 2019, **12**, 559–572.
30 P. Wu, S. Zhang, H. Yang, Y. Zhu and J. Chen, *J. Polym. Sci., Part A:Polym. Chem.*, 2018, **56**, 1508–1515.
31 X. Su, H. Li, X. Lai, L. Zhang, X. Liao, J. Wang, Z. Chen, J. He and X. Zeng, *ACS Appl. Mater. Interfaces*, 2018, **10**, 4213–4221.
32 Q. Wei, O. Oribayo, X. Feng, G. L. Rempel and Q. Pan, *Ind. Eng. Chem. Res.*, 2018, **57**, 8918–8926.
33 H. Ahmad, M. K. Hasan, M. A. J. Miah, A. M. I. Ali and K. Tauer, *Polymer*, 2011, **52**, 3925–3932.
34 Z. C. Ng, R. A. Roslan, W. J. Lau, M. Gürsoy, M. Karaman, N. Jullok and A. F. Ismail, *Polymers*, 2020, **12**, 1883.
35 J.-O. Jeong, J.-S. Park and Y.-M. Lim, *Materials*, 2016, **9**, 441.
36 L. Liang, Y. Xue, Q. Wu, Y. Dong and X. Meng, *RSC Adv.*, 2019, **9**, 40378–40387.
37 S. M. Kong, Y. Han, N. Il Won and Y. H. Na, *ACS Omega*, 2021, **6**, 33969–33975.
38 K. Maghsoudi, G. Momen and R. Jafari, *Appl. Mater. Today*, 2023, **34**, 101893.
39 S. Parvate, P. Dixit and S. Chattopadhyay, *J. Phys. Chem. B*, 2020, **124**, 1323–1360.
40 P. Forsberg, F. Nikolajeff and M. Karlsson, *Soft Matter*, 2011, **7**, 104–109.
41 O. Şanli and E. Pulat, *J. Appl. Polym. Sci.*, 1993, **47**, 1–6.
42 J. Jang and B.-S. Kim, *J. Appl. Polym. Sci.*, 2000, **77**, 903–913.
43 W.-L. Liu, S. Lirio, Y. Yang, L.-T. Wu, S.-Y. Hsiao and H.-Y. Huang, *J. Chromatogr. A*, 2015, **1395**, 32–40.

44 E. Grushevenko, T. Rokhmanka, S. Sokolov, A. Basko, I. Borisov, K. Pochivalov and A. Volkov, *Polymers*, 2023, **15**, 4436.
45 B. Wu, W. Chassé, A. Heise, A. P. M. Kentgens, D. F. Brougham and V. M. Litvinov, *Mater. Chem. Front.*, 2022, **6**, 990–1004.
46 I. Barbarin, N. Politakos, L. Serrano Cantador, J. A. Cecilia, O. Sanz and R. Tomosvka, *ACS Appl. Polym. Mater.*, 2022, **4**, 9065–9075.
47 A. Rawat and D. J. Burgess, *Int. J. Pharm.*, 2010, **394**, 99–105.
48 H. Gui, J. Chen, T. Yang, S. Zuo, X. Li, C. Yao and F. Liang, *Langmuir*, 2023, **39**, 9865–9874.
49 J. Zhang, X. Liu, F. Chen, J. Liu, Y. Chen, F. Zhang and N. Guan, *J. Dispersion Sci. Technol.*, 2020, **41**, 1136–1144.
50 N. Hendeniya, S. T. Mahmud, S. Abtahi and B. S. Chang, *Macromolecules*, 2026, **59**, 3477–3486.
51 J. A. Emerson, D. T. W. Toolan, J. R. Howse, E. M. Furst and T. H. Epps, *Macromolecules*, 2013, **46**, 6533–6540.
52 S. Chatterjee, P. Doshi and G. Kumaraswamy, *Soft Matter*, 2017, **13**, 5731–5740.
53 J. Martinez, M. Aghajani, Y. Lu, A. K. Blevins, S. Fan, M. Wang, J. P. Killgore, S. B. Perez, J. Patel, C. Carbrello, S. Foley, R. Sylvia, R. Long, R. Castro and Y. Ding, *J. Membr. Sci.*, 2022, **641**, 119898.
54 P. Jiang, K. Li, X. Chen, R. Dan and Y. Yu, *Appl. Sci.*, 2020, **10**, 1453.
55 H. Meng, T. Yan, J. Yu and F. Jiao, *Chin. J. Chem. Eng.*, 2018, **26**, 957–963.
56 J. Li, D. Li, W. Hu, J. Li, Y. Yang and Y. Wu, *New J. Chem.*, 2015, **39**, 9958–9962.
57 J. Wang and G. Geng, *Mar. Pollut. Bull.*, 2015, **97**, 118–124.
58 N. Cao, B. Yang, A. Barras, S. Szunerits and R. Boukherroub, *Chem. Eng. J.*, 2017, **307**, 319–325.
59 S. Liu, Q. Xu, S. S. Latthe, A. B. Gurav and R. Xing, *RSC Adv.*, 2015, **5**, 68293–68298.
60 G. Wang, Z. Zeng, X. Wu, T. Ren, J. Han and Q. Xue, *Polym. Chem.*, 2014, **5**, 5942–5948.
61 M. Khosravi and S. Azizian, *ACS Appl. Mater. Interfaces*, 2015, **7**, 25326–25333.
62 Z. Kong, J. Wang, X. Lu, Y. Zhu and L. Jiang, *Nano Res.*, 2017, **10**, 1756–1766.